
Nonmyopic Multiclass Active Search for Diverse Discovery

Quan Nguyen¹ Roman Garnett¹

Abstract

Active search is a setting in adaptive experimental design where we aim to uncover members of rare, valuable class(es) subject to a budget constraint. An important consideration in this problem is diversity among the discovered targets – in many applications, diverse discoveries offer more insight and may be preferable in downstream tasks. However, most existing active search policies either assume that all targets belong to a common positive class or encourage diversity via simple heuristics. We present a novel formulation of active search with multiple target classes, characterized by a utility function that naturally induces a preference for label diversity among discoveries via a diminishing returns mechanism. We then study this problem under the Bayesian lens and prove a hardness result for approximating the optimal policy. Finally, we propose an efficient, nonmyopic approximation to the optimal policy and demonstrate its superior empirical performance across a wide variety of experimental settings, including drug discovery.

1. Introduction

A theme underlying many real-world applications is the need to rapidly discover rare, valuable instances from massive databases in a budget-efficient manner. For example, both drug discovery and fraud detection entail searching through huge spaces of candidates for rare instances exhibiting desired properties: binding activity against a biological target for drug discovery, or fraudulent behavior for fraud detection. However, in both of these cases, labeling a given data point is exceptionally expensive: synthesis and characterization in a laboratory for drug discovery, and human intervention (and possibly lost sales) for fraud detection. This extreme cost of labeling rules out exhaustive scanning and raises a challenge in experimental design. The *active search* (AS) framework frames such tasks in terms of active

learning, where one iteratively queries an expensive oracle to determine whether chosen data points are valuable. The goal of AS is then to design an adaptive policy for selecting queries to send to the oracle in order to identify as many valuable data points as possible under a given budget.

AS has enjoyed a great deal of study (Garnett et al., 2012; Jiang et al., 2017; 2018; 2019; Nguyen et al., 2021), and strong theoretical results and efficient algorithms are known. Most relevant to this work, Jiang et al. (2017) established a strong hardness result for AS. Namely, *no* computationally tractable policy (i.e., one that runs in polynomial time with respect to its querying budget) can guarantee recovery within any constant factor of the (exponential-time) optimal policy in the worst case. This proof was by an explicit construction of arbitrarily hard problems. Nonetheless, Jiang et al. (2017) were also able to develop an efficient, nonmyopic policy that achieves impressive empirical results.

This study and the others cited above all operate under a binary setting where every data point under consideration is either valuable or not. The total number of discoveries made in a given budget is then used as a utility function during experimental design, encoding equal marginal utility for every discovery made. However, this may not adequately capture preferences over experimental outcomes in many practical scenarios, where there may be *diminishing returns* in finding additional members of a frequently observed class. This is the case in, e.g., scientific discovery, where a discovery in a completely novel region of the design space may offer more marginal insight than the 100th discovery in a region already known to contain many valuable items. In this work, we will consider a *multiclass* variant of the AS problem, wherein discoveries in a particularly rare class are awarded more marginal utility than those in an already well-covered class. As we will see, this approach naturally encourages *diversity* among the points discovered by the policy.

After defining this problem, we proceed to study it through the lens of Bayesian decision theory and make two main contributions. First, we extend the hardness of approximation result by Jiang et al. (2017) to our setting, proving that multiclass AS is also a fundamentally difficult problem. Second, we propose an approximation to the optimal policy that is both computationally efficient and nonmyopic. We demonstrate that our policy effectively encourages diversity

¹Washington University in St. Louis, MO, USA. Correspondence to: Quan Nguyen <quan@wustl.edu>.



Figure 1. Number of discoveries by region relative to a uniform target distribution by the state-of-the-art policy under linear utility ENS, in a toy search problem where points within the visible regions in the unit square are considered search targets. ENS oversamples the center region, the most common and easiest-to-identify target class, and thus collects a highly unbalanced dataset.

among discoveries returned from the search. Further, similar to nonmyopic policies from previous work, we show that our policy leverages budget-awareness to dynamically balance between exploration and exploitation during the search. We demonstrate the superior empirical performance of our proposed algorithm through an exhaustive series of experiments, including a challenging drug discovery setting. Across the board, our proposed policy recovers both better balanced and richer datasets than a suite of strong baselines.

2. Problem Definition

We first introduce the multiclass active search problem with diminishing returns and present the Bayesian optimal policy. This policy will be hard to compute (or even approximate), but will inspire the algorithm developed in the next section. Suppose we are given a large but finite set of points $\mathcal{X} \triangleq \{x_i\}$, each of which belongs to exactly one of C classes, denoted by $[C] \triangleq \{1, 2, \dots, C\}$, where $C > 2$. We assume class-1 instances are abundant and uninteresting, while other classes are rare and valuable; we call the members of these classes *targets*. The class membership of a given point $x \in \mathcal{X}$ is not known *a priori* but can be determined by making a query to an oracle that returning its label $y = c$. We assume this labeling procedure is expensive and can only be accessed a limited number of times $T \ll n \triangleq |\mathcal{X}|$ – the querying budget. Denote a given dataset of queried points and labels as $\mathcal{D} = \{(x_i, y_i)\}$, and \mathcal{D}_t as the dataset collected after t queries to the oracle in a given search.

Our high-level goal is to design a policy that decides which elements of \mathcal{X} should be queried in order to uncover as many targets as possible. Preferences over over different datasets (experimental outcomes) are expressed via a *utility function*; previous work (Garnett et al., 2012; Jiang et al.,

2017) has used a linear utility in the binary setting $C = 2$:

$$u(\mathcal{D}) = \sum_{y \in \mathcal{D}} \mathbb{1}\{y > 1\}.$$

Under our model, this effectively groups all targets in a common positive class and assigns equal reward to each target discovery.

In many practical scenarios, however, once a target class has been thoroughly investigated, the marginal utility of finding yet more examples decreases and we would prefer to either expand a rarely sampled class or discover a new one. For example, in drug discovery – one of the main motivating applications for AS – screening procedures that are simply optimized for hit rate tend to propose very structurally similar compounds and lead to an overall decline in usefulness of these discoveries downstream (Galloway et al., 2010). This has led to efforts to artificially encourage diversity when generating new screening experiments, as a way to induce the desired search behavior (Benhenda, 2017; Pereira et al., 2021).

The preferences described above reflect the notion of *diminishing returns*. We propose to capture diminishing returns for marginal discoveries in a known class (and thereby encourage diversity in discoveries) by a logarithmic reward function for each class:

$$\begin{aligned} u(\mathcal{D}) &\triangleq \sum_{c>1} \log \left(1 + \sum_{y \in \mathcal{D}} \mathbb{1}\{y = c\} \right) \\ &= \sum_{c>1} \log(1 + m_c), \end{aligned} \quad (1)$$

where m_c is the number of targets of class c in \mathcal{D} . We will also use $m_{c,t}$ to denote the corresponding number in \mathcal{D}_t .

Under this model, the marginal gain of an additional discovery decreases with the size of the corresponding class in \mathcal{D} . This effectively rewards label diversity within the collected targets: across different datasets \mathcal{D} with the same number of targets, utility is maximized when the target counts across the valuable classes are equal, i.e., $m_2 = \dots = m_C$.

Consider a toy problem illustrated in Fig. 1, where we wish to search for points close to the center and corners of the unit square, each representing a target class. The state-of-the-art ENS policy by Jiang et al. (2017) under linear utility recovers many targets, but over-exploits the center region where targets are most plentiful. This is an undesirable behavior with respect to our diversity objective, which would prefer to have discoveries balanced across all classes. We will develop policies achieving this balance in the next section.

2.1. The Bayesian Optimal Policy

We now derive the optimal policy in the expected case using Bayesian decision theory. To do this, we first assume access

to a probabilistic classification model that computes the posterior probability that a point $x \in \mathcal{X}$ belongs to class $c \in [C]$ given an observed dataset \mathcal{D} , denoted by $p_c(x | \mathcal{D}) \triangleq \Pr(y = c | x, \mathcal{D})$. (We sometimes omit the dependence on \mathcal{D} in the notation when the context is clear.) This model may be arbitrary.

Suppose we are currently at iteration $t + 1 \leq T$, having collected dataset \mathcal{D}_t , and now need to identify the next point $x_{t+1} \in \mathcal{X} \setminus \mathcal{D}_t$ to query the oracle with. The optimal policy selects the point that maximizes the expected utility of the *terminal* dataset \mathcal{D}_T , conditioned on the current query, recursively assuming that future queries will also be made optimally:

$$x_{t+1}^* = \arg \max_{x_{t+1} \in \mathcal{X} \setminus \mathcal{D}_t} \mathbb{E}[u(\mathcal{D}_T) | x_{t+1}, \mathcal{D}_t]. \quad (2)$$

This expected optimal utility may be computed using backward induction (Bellman, 1957). In the base case where $t = T - 1$ and we are faced with the very last query x_T ,

$$\mathbb{E}[u(\mathcal{D}_T) | x_T, \mathcal{D}_{T-1}] = \sum_{c \in [C]} u(\mathcal{D}_T) p_c(x_T | \mathcal{D}_{T-1}).$$

Maximizing this expectation is equivalent to maximizing the expected *marginal utility gain*

$$\begin{aligned} \Delta(x_T | \mathcal{D}_{T-1}) &\triangleq \sum_{c > 1} p_c(x_T | \mathcal{D}_{T-1}) \times \\ &\times \left[\log(2 + m_{c,T-1}) - \log(1 + m_{c,T-1}) \right]. \end{aligned} \quad (3)$$

It may be observed that for each class index c , this quantity not only increases as a function of the positive probability p_c , but also decreases as a function of the number of targets already found in that class. Therefore, even at this very last step, the optimal decision balances between hit probability and discovery/extension of a rare class.

When more than one query remains in our budget, the expected optimal utility in Eq. (2) expands into

$$\begin{aligned} \mathbb{E}[u(\mathcal{D}_T) | x_{t+1}, \mathcal{D}_t] &= u(\mathcal{D}_t) + \Delta(x_{t+1} | \mathcal{D}_t) + \\ &\mathbb{E}_{y_{t+1}} \left[\max_{x_{t+2}} \mathbb{E}[u(\mathcal{D}_T) | x_{t+2}, \mathcal{D}_{t+1}] - u(\mathcal{D}_{t+1}) \right], \end{aligned}$$

where $\mathbb{E}[u(\mathcal{D}_T) | x_{t+2}, \mathcal{D}_{t+1}]$ is the expected utility that is a step further into the future and may be recursively computed using the same expansion. Here, we note while the first term in the sum on the right-hand side (the utility at the current step $u(\mathcal{D}_t)$) is a constant, the other two terms may be interpreted as balancing between exploitation from the immediate reward (the marginal gain $\Delta(x_{t+1} | \mathcal{D}_t)$), and exploration from the future rewards to be optimized by subsequent queries (the expected future utility).

Overall, computing this expectation involves $(\ell - 1)$ further nested expectations and maximizations, where $\ell = T - t$ is the search horizon. This has a time complexity of $O((Cn)^\ell)$, making finding the optimal decision intractable for any large dataset. A potential solution to this problem is to limit the lookahead horizon by pretending that ℓ is small, thus myopically approximating the optimal policy. The simplest form of this is to set $\ell = 1$ and greedily optimize for the one-step expected marginal utility gain in Eq. (3). We will refer to the resulting policy as the one-step policy.

Since our utility function has elements with diminishing returns, a question naturally arises as to whether the results from the submodularity (Krause & Guestrin, 2007) and adaptive submodularity (Golovin & Krause, 2011) literature apply here, and whether the greedy strategy of the one-step policy could approximate the optimal policy well. In the next subsection, we present the perhaps surprising result that *no* polynomial-time policy can approximate the optimal policy by any constant factor.

2.2. Hardness of Approximation

Assuming that a given policy only has access to a unit-cost conditional probability $p_c(x | \mathcal{D})$ for any point $x \in \mathcal{X}$ and dataset \mathcal{D} , we obtain the same hardness result of Jiang et al. (2017) under our new utility model:

Theorem 2.1. *There is no polynomial-time policy with a constant factor approximation ratio for optimizing the expected utility.*

Our proof strategy closely follows that of Jiang et al. (2017). We construct a family of hard problem instances, where in each instance a secret set of points encodes the location of a larger “treasure” of targets. The probability of successfully discovering this treasure is extremely small without observing the secret set first, which in itself is vanishingly unlikely to happen under polynomial time. Further, the average hit rate outside of the treasure set is vanishingly low, making it infeasible to compete with the optimal policy. The complete proof is included in Appx. A.

Despite this negative result, we can still hope to design search policies that are *empirically* effective. In the next section, we propose an efficient, nonmyopic approximation to the optimal policy that we will show works well in practice.

3. Efficient Nonmyopic Approximation

Our proposed policy extends the ENS heuristic introduced under the binary setting by Jiang et al. (2017). The key idea is to assume that after a proposed query in the current iteration, all remaining budget will be spent *simultaneously* on a single batch of queries exhausting the budget. This assumption simplifies the decision tree we must analyze,

reducing its depth to 2 while expanding the branching factor of the last layer. However, under the linear utility model, the expected marginal utility of a final batch of queries conveniently decomposes into a sum of positive probabilities of individual batch members. The optimal final batch therefore consists of the points with the highest probabilities, which may be computed efficiently. Further, by matching the size of the following batch to the number of queries remaining, we can effectively account for our remaining budget when computing the expected utility of a given putative query.

Unfortunately, the linear decomposition enabling rapid computation in ENS does not hold in our setting due to our nonlinear utility (1), and designing an effective batch policy requires more care. We present our solution below.

3.1. Making a Batch of Queries

We first temporarily consider the subproblem of designing a batch of b queries X given a dataset \mathcal{D} , so as to maximize the expected utility of the combined observation set, i.e., $\mathbb{E}_Y [u(\mathcal{D} \cup X, Y)]$, where the expectation is taken over Y ,¹ the labels of the points in X . As labels may be conditionally dependent and the utility function u is not linear, exact computation of this expectation requires iterating over all C^b realizations of the label set Y . This is infeasible unless b is very small, and represents the primary challenge we must overcome.

A crude but effective mechanism to address the conditional dependence of labels is to simply assume conditional independence. This relieves us from having to update the posterior probabilities of remaining points given fictitious observations arising in the computation. Interestingly, under this assumption, ENS in fact represents the *optimal* policy given the linear utility. However, under our setting, even if we assume conditional independence, we still face challenges in computing the expected utility:

$$\mathbb{E}_Y [u(\mathcal{D} \cup X, Y)] = \sum_{c>1} \mathbb{E}_Y [\log(1 + m'_c)], \quad (4)$$

where m'_c is the total number of targets belonging to class c in the union set of \mathcal{D} and a particular realization of Y .

Our solution is to use Jensen’s inequality to obtain an upper bound on the expected utility:

$$\begin{aligned} \mathbb{E}_Y [u(\mathcal{D} \cup X, Y)] &= \sum_{c>1} \mathbb{E}_Y [\log(1 + m'_c)] \\ &\leq \sum_{c>1} \log(\mathbb{E}_Y [1 + m'_c]). \end{aligned}$$

¹In this section, expectations over Y are universally conditioned on knowledge of X and \mathcal{D} ; we drop this conditioning from the expressions to clarify the main ideas.

Now, for a given c , the inner expectation may be rewritten as the sum of probabilities (and some constants):

$$\mathbb{E}_Y [1 + m'_c] = 1 + m_c + \sum_{x \in X} p_c(x | \mathcal{D}).$$

We then upper-bound the overall expected utility:

$$\begin{aligned} \mathbb{E}_Y [u(\mathcal{D} \cup X, Y)] &\leq \bar{u}(X) \\ &\triangleq \sum_{c>1} \log\left(1 + m_c + \sum_{x \in X} p_c(x | \mathcal{D})\right). \end{aligned}$$

We propose to use this upper bound, \bar{u} , to approximate the expected utility of a batch for the purposes of policy computation. In Appx. B, we present simulation results comparing the fidelity of this approximation to that of Monte Carlo sampling. Overall, our method offers competitive accuracy even against sampling with a large number of samples of Y (>1000), while being significantly more computationally lightweight. Here, speed is paramount since under the ENS heuristic, computing the utility of a batch is a subroutine that needs to run many times (C times for each putative query candidate, once for each putative label). Another attractive feature of our approach is that \bar{u} is a monotone submodular set function, which will facilitate (approximate) maximization.

At this point, our goal is to find the batch X that maximizes \bar{u} , as an approximation to the batch maximizing the expected one-step marginal utility. Naïvely maximizing \bar{u} requires iterating over all $\binom{n}{b}$ candidate batches to compute the corresponding score. However, we note that the score is a sum of log functions, which are monotone submodular, and therefore \bar{u} is a monotone submodular function itself. As such, we opt to *greedily* optimize \bar{u} by sequentially maximizing the pointwise marginal gain; the resulting batch provides a $(1 - 1/e)$ -approximation for the optimal batch (Nemhauser et al., 1978; Krause & Guestrin, 2007).

We briefly remark on the nature of the batches resulting from this greedy procedure, which naturally encourages batch members to be diverse in their likely labels: once a point having a high p_c is added to X , others with high $p_{c'}$ for another target will be prioritized during the next selection. This is a desideratum of a batch policy given our diversity-encouraging objective, indicating the output of the algorithm is a reasonable approximation of the optimal batch. Further, when $b = 1$ (that is, we are at the second-to-last iteration), this procedure guarantees we will make the true expected-case optimal decision – a reassuring feature.

3.2. Completing the Algorithm

With a method of constructing approximate one-step optimal batches in hand, we now follow the ENS heuristic to complete our proposed policy, *diversity-aware active search*,

Algorithm 1 Diversity-aware active search (DAS)

inputs observations \mathcal{D}_t , remaining budget $T - t$
returns x_{t+1}^* maximizing the score in Eq. (5)
for $x_{t+1} \in \mathcal{X} \setminus \mathcal{D}_t$ **do**
 for $y_{t+1} \leftarrow 1$ **to** C **do**
 $f(x_{t+1} | y_{t+1}) \leftarrow \bar{u}(X | \mathcal{D}_t \cup \{(x_{t+1}, y_{t+1})\})$
 end for
 $f(x_{t+1}) \leftarrow \sum_c p_c(x_{t+1}) f(x_{t+1} | c)$
end for
 $x_{t+1}^* \leftarrow \arg \max_{x_{t+1}} f(x_{t+1})$

or DAS. For a candidate observation x_{t+1} , we condition on each possible label $y_{t+1} \in [C]$ for this point, approximate the optimal batch observation following (x_{t+1}, y_{t+1}) , and average the resulting approximate terminal utility \bar{u} over the labels:

$$f(x_{t+1}) = \mathbb{E}_{y_{t+1}} [\bar{u}(X) | x_{t+1}, \mathcal{D}_t], \quad (5)$$

where \bar{u} depends on the putative data $\mathcal{D} \cup (x_{t+1}, y_{t+1})$. DAS proceeds by selecting the candidate x_{t+1}^* that maximizes f . This procedure is summarized in Alg. 1.

As mentioned, with the lookahead batch construction simulating future queries, DAS accounts for not only the immediate reward but also the impact of the chosen query on future rewards. Additionally, the latter quantity naturally decreases as a function of the remaining budget b , allowing our policy to be budget-aware and dynamically balance exploitation and exploration without any tradeoff parameter.

We briefly demonstrate the benefits of our approach by continuing with the example problem previously seen in Fig. 1, where the ENS policy, in seeking to maximize only recovery, collected highly unbalanced datasets. Fig. 2 shows the results of the one-step policy and DAS under the same setting. Compared to ENS, one-step distributes its queries more equally among the regions, but it is our proposed policy DAS that constructs the most diverse dataset. Over the 20 repeated simulations that we run, DAS achieves the best average utility of 14.25 ± 0.07 , compared to ENS’s 11.88 ± 0.40 and one-step’s 13.14 ± 0.24 .

3.3. Implementation and Pruning

A naïve implementation of the batch subroutine in DAS has a complexity of $O(bn)$, and the entire DAS procedure thus has a complexity of $O(Cn(bn)) = O(Cbn^2)$, where again $n = |\mathcal{X}|$ is the size of our search space and b is the remaining budget. We discuss in this subsection several strategies that allow our method to scale to large datasets.

We first describe the k -NN model used in our experiments, first introduced by Garnett et al. (2012) in the binary setting. The idea is to use the proportion of class- c members among

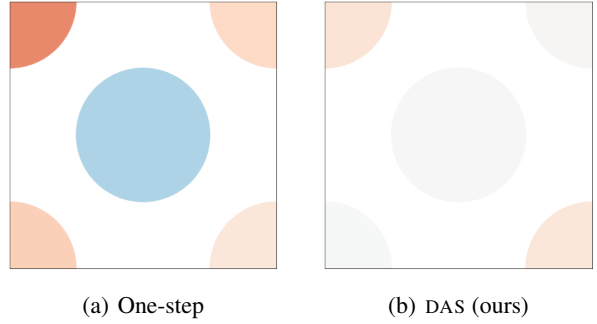


Figure 2. Number of discoveries by region relative to a uniform target distribution by the one-step optimal policy and our proposal DAS, in the same problem visualized in Fig. 1. One-step distributes its queries more equally than the previously seen ENS; however, center points are still somewhat over-represented. On the other hand, DAS constructs more diverse datasets and finds more rare targets in the corners.

the observed nearest neighbors of a given point x as the posterior marginal probability $p_c(x | \mathcal{D})$. Formally, denote the set of nearest neighbors of x as $\text{NN}(x)$ and the (potentially empty) subset of labeled neighbors as $\text{LNN}(x) \subseteq \text{NN}(x)$. Then, the posterior probability of x belonging to class c is

$$p_c(x | \mathcal{D}) = \frac{\gamma_c + \sum_{x' \in \text{LNN}(x)} \mathbb{1}\{y' = c\}}{1 + |\text{LNN}(x)|},$$

where each $\gamma_c \in (0, 1)$ is a hyperparameter acting as a “pseudocount”, or our prior belief about the prevalence of class c (since $p_c(x | \mathcal{D}) = \gamma_c$ if $\text{LNN}(x) = \emptyset$). These pseudocounts add up to 1.

This k -NN achieves reasonable generalization error in practice (in the sparsely labeled setting we are considering here), and can be rapidly updated given a new observation, which is a valuable feature with respect to our method. Another benefit is that it is possible to cheaply compute a *posterior probability upper bound* p^* , given any dataset \mathcal{D} and an additional observation with label y :

$$\max_{x' \in \mathcal{X} \setminus \mathcal{D}} p_c(x' | \mathcal{D} \cup \{(x, y)\}) \leq p_c^*(y, \mathcal{D}).$$

This upper bound is useful in that we may then bound the approximate expected terminal utility \bar{u} conditioned on label c when computing the score in Eq. (5), i.e., $f(x | y = c)$, and therefore the overall score $f(x)$. With these score upper bounds in hand, we employ branch-and-bound pruning strategies used in previous work (Jiang et al., 2018; Nguyen et al., 2021). Briefly, before evaluating the score f of a given candidate x , we compare the upper bound of $f(x)$ against the current best score f^* that we have found. If f^* exceeds this upper bound, computing $f(x)$ is no longer necessary and we simply proceed to the next candidate. Otherwise, since we also have access to the *conditional*

score upper bounds for $f(x | y = c)$, as we marginalize over each label y , we further check whether the conditional scores computed thus far, when combined with the complementary conditional upper bounds, are less than f^* . If this is the case, we terminate the current f computation “on the fly.” The upper bounds p_c^* are cheap to evaluate, and these checks add a trivial overhead to the entire procedure in the pessimistic situation of no pruning – in practice, this cost is well worth it. Finally, a lazy-evaluation strategy is used, where candidates are evaluated in descending order of their score upper bounds, so that a given point that may be pruned will not be evaluated.

So far, these methods are used in the outer loop of DAS. We also employ a pruning strategy for the inner batch-building procedure. First, observe that in this procedure, points having the same marginal probabilities p_c (conditioned on a putative query) are interchangeable as we have assumed conditional independence. We point out one particular set of such points with equal p_c : those whose marginal probabilities have not been updated from the prior due to having no labeled nearest neighbors. In a typical AS iteration, there may be many such points, especially in early stages of the search. Pruning duplicates appropriately allows the follow-on batch to be built more efficiently, and we empirically observed a drastic improvement in our experiments. A welcome property of this method is that it has the most impact in the early iterations of a search, which would usually be the longest-running iterations otherwise.

Overall, the combination of these strategies allows our algorithm to scale to large datasets ($>100\,000$ points), as we will see shortly.

4. Related Work

Active search, first proposed by Garnett et al. (2012), is a variant of active learning (AL) (Settles, 2009) where we aim not to learn an accurate model, but to collect members of rare and valuable classes. Previous work has explored AS under a wide range of settings, such as when the goal is to hit a targeted number of positives as quickly/cheaply as possible (Warmuth et al., 2002; 2003; Jiang et al., 2019), when queries are to be made in batches (Jiang et al., 2018), or with multifidelity oracles (Nguyen et al., 2021). These investigations all assumed that there is only one target class, and collecting a target constitutes a constant reward. Our work is the first to our knowledge to tackle multiclass AS using principled Bayesian decision theory.

Diversity as an objective has enjoyed great interest from the broader AL community. A common approach is to modify a typical AL acquisition function to encourage diversity in the resulting queries. For example, Gu et al. (2015) and Yang et al. (2015) encouraged diversity by incorporating

dissimilarity terms (computed via an RBF kernel) into uncertainty sampling schemes. Brinker (2003) meanwhile used the angles between the hyperplanes induced by adding new points to the training set of an SVM, and Zhdanov (2019) considered the minimum distance between any pair of labeled points. Others have employed coreset-based strategies (Sener & Savarese, 2018; Agarwal et al., 2020) to identify a set of representative points with a high level of diversity. Another popular strategy is to partition a given dataset into different groups (e.g., using a clustering algorithm) and inspect the groups in a round-robin manner (Madani et al., 2004; Lin et al., 2018; Ma et al., 2020; Citovsky et al., 2021). We will also apply a round-robin heuristic to a number of benchmarks in our experiments.

He & Carbonell (2007) studied a related problem where the objective is to detect at least one instance of each rare target class as quickly as possible. By assuming the target classes are highly concentrated, they design a policy that optimizes the difference in local density between a given point and its nearest neighbors, which is effective at identifying targets on the boundary. Malkomes et al. (2021) considered the *constraint active search* problem, in which they seek to find a diverse set of points satisfying a set of constraints. The authors propose maximizing the expected improvement in a coverage measure given a new observation. The strategies employed by these studies are the one-step optimal policies under their respective utility functions. As we will see shortly, the analogous one-step policy in our setting is greatly outperformed by our nonmyopic proposal, demonstrating there is value in going beyond one-step lookahead.

Diversity has also been explored in the related task of Bayesian optimization (Garnett, 2022). A common approach is to incorporate a determinantal point process (Kulesza & Taskar, 2012) to induce diversity in the feature space (Wang et al., 2018; Nava et al., 2021). In the multiobjective setting, many policies reason about the diversity of their collected data in the Pareto space and leverage this knowledge to design queries (Gupta et al., 2018; Shu et al., 2020; Lukovic et al., 2020).

5. Experiments

We perform a wide range of experiments to demonstrate the empirical performance of our policy DAS and present our results in this section. First, we discuss the benchmarks used. We have already mentioned the one-step policy, which greedily maximizes the marginal utility at each iteration. Another baseline is ENS (Jiang et al., 2017), which provides state-of-the-art performance for the binary setting, where we simply lump all targets into a single positive class.

We also consider a family of policies that design queries in a *round-robin* (RR) manner. Here, in each iteration t we

Table 1. Average search utility and standard errors across 20 repeated experiments for each setting. C is the total number of unique classes in the search space. The best performance in each column is highlighted in **bold**; policies that are not significantly worse than the best (according to a two-sided paired t -test with a significance level of $\alpha = 0.05$) are in *blue italics*.

	CiteSeer ^x		Drug Discovery		
	$C = 5$	$C = 10$	$C = 5$	$C = 10$	$C = 15$
ENS	16.57 (0.08)	32.54 (0.50)	10.29 (0.68)	13.79 (0.85)	17.00 (1.15)
RR-greedy	16.66 (0.14)	33.08 (0.13)	10.87 (0.82)	18.66 (1.13)	24.87 (0.95)
RR-UCB	16.68 (0.12)	33.22 (0.13)	11.60 (0.90)	19.27 (1.13)	26.45 (0.96)
	$(\beta^* = 1)$	$(\beta^* = 3)$	$(\beta^* = 3)$	$(\beta^* = 3)$	$(\beta^* = 10)$
RR-ENS	17.47 (0.11)	33.78 (0.16)	10.56 (0.72)	17.83 (0.66)	23.58 (0.88)
One-step	16.77 (0.13)	34.01 (0.13)	11.68 (0.92)	19.06 (0.98)	27.40 (1.11)
DAS (ours)	<i>17.37 (0.09)</i>	34.45 (0.11)	13.34 (0.79)	23.39 (0.83)	31.48 (1.25)

choose a target class c_t and seek to make a discovery for this target class. A round-robin policy then continually rotates the target class among the positive classes throughout the search, devoting an equal amount of resources to each class.

The first of these policies is RR-greedy, which for a given class index c_t queries the point that maximizes the probability p_{c_t} . Another round-robin baseline is RR-UCB, which maximizes an upper confidence bound score (Auer, 2002) corresponding to c_t : $p_{c_t} + \beta \sqrt{p_{c_t}(1 - p_{c_t})}$. Here β is a hyperparameter trading off exploitation (class membership probability) and uncertainty (as measured by the standard deviation of the binary indicator $[y = c_t]$). We evaluate this policy for $\beta \in \{0.1, 0.3, 1, 3, 10\}$ and report the result of the best performing value of β , denoted β^* in our results (Tab. 1). Finally, we consider RR-ENS, which applies the ENS heuristic to the subproblem of finding positives in the target class c_t . As the remaining budget will be equally allocated among the positive classes, we adjust the remaining budget when constructing lookahead batches accordingly.

Under each experimental setting described below, we set our budget $T = 500$ and run our policies 20 times, each with an initial dataset of a randomly selected target.

5.1. The CiteSeer^x Dataset

For our first large-scale experiment, we use the CiteSeer^x citation network data, introduced by Garnett et al. (2012). This dataset contains 39 788 papers that were published at the 50 most popular computer science conferences and journals, and the label of each paper is its publication venue. First, an undirected citation network is formed, and from there the feature vector of each point is computed via graph principal component analysis (Fouss et al., 2007) on the network; we keep the first 20 components.

Our overall goal is to search for papers in machine learning and artificial intelligence proceedings. To this end, we

conduct two sets of experiments with different numbers of classes C . For $C = 5$, we select papers from NeurIPS, ICML, UAI, and JMLR as our four target classes, adding up to 5575 targets (roughly 14% hit rate; an average of 3.5% per class). For $C = 10$, we additionally include papers from IJCAI, AAAI, JAIR, Artificial Intelligence, and Machine Learning as targets. This totals 12 382 targets, yielding a 31% overall hit rate and again a 3.5% per class. We do not test for larger values of C to avoid increasing the total hit rate and violating the assumption about rare target classes. The average utility and standard errors of the considered policies across 20 repeats are shown in the first two columns of Tab. 1.

5.2. Drug Discovery

We further experiment with a drug discovery task using a massive chemoinformatic dataset. The goal is to identify chemical compounds that exhibit selective binding activity given a specific protein. Our dataset consists of 120 such activity classes from BindingDB (Liu et al., 2007). For each activity class, there are a small number of compounds with significant binding activity – these are our search targets.

In each experiment for a given value $C \in \{5, 10, 15\}$, we select $(C - 1)$ out of the 120 classes uniformly at random without replacement to form the target classes. They are then combined with 100 000 points sampled from the “drug-like” entries in the ZINC database (Sterling & Irwin, 2015), which serve as the negative set, to make up our search space. Features for these points are binary vectors encoding chemical properties, typically referred to as fingerprints. We use the Morgan fingerprint (Rogers & Hahn, 2010), which has shown good performance in past studies.

The average prevalence of a target is 0.2%; the total hit rates are thus 1%, 2%, and 3% for $C = 5, 10,$ and 15, respectively. We report the performance of our policies in the last three columns of Tab. 1.

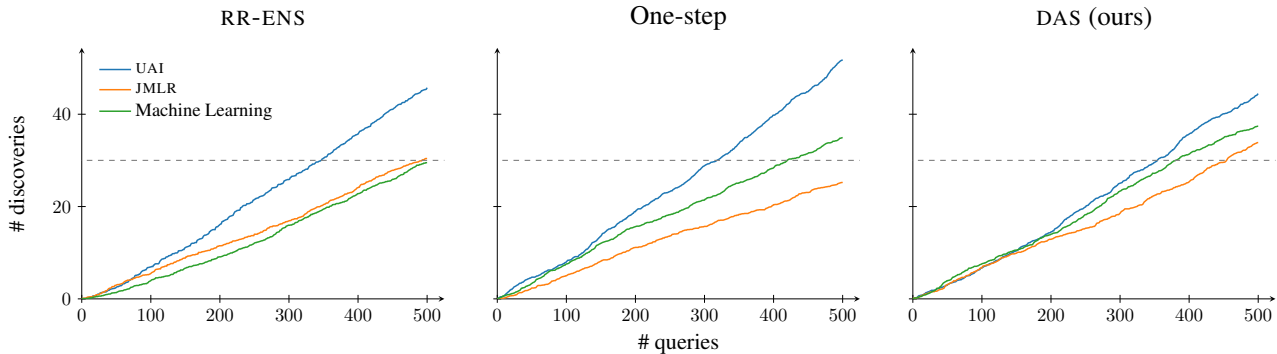


Figure 3. Average count of least-common papers found by different active search policies across the CiteSeer^x $C = 10$ experiments. DAS finds more members of rare classes than other policies.

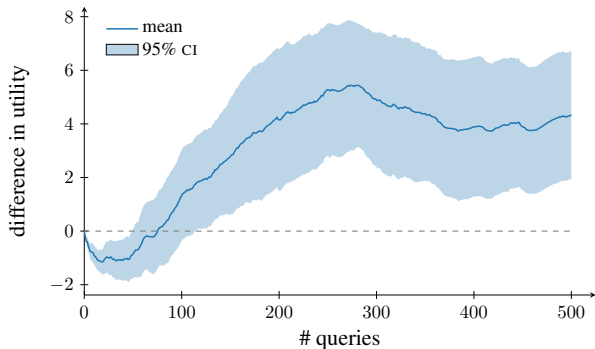


Figure 4. Average difference in cumulative reward between DAS and one-step across the drug discovery $C = 10$ experiments. DAS dynamically balances exploration and exploitation.

5.3. Discussion

Overall, DAS is the consistent winner across all but one setting we investigated (CiteSeer^x with $C = 5$), where its performance is not significantly worse than the best policy. This consistent performance highlights the benefits of our nonmyopic, budget-aware approach. The one-step policy is usually the second-best among the baselines, demonstrating even a greedy strategy within our decision-theoretic framework is typically more effective than the other heuristics we consider. Inspecting the optimal values for RR-UCB’s trade-off parameter β^* , we notice a natural trend: as C increases, so does the need for exploration, and larger values of β are thus selected.

To further demonstrate that DAS is effective at constructing *diverse* observations, we show in Fig. 3 the average numbers of discoveries made by the three best-performing policies under the CiteSeer^x $C = 10$ experiments for the three least-common classes: UAI (792 in total), JMLR (739), and Machine Learning (679) papers. We observe that DAS successfully finds more targets belonging to the rarer classes of JMLR and Machine Learning, with a better balance among these classes as well.

By construction, DAS is aware of its remaining budget at any

time during a search and therefore could dynamically balance between exploration and exploitation. We demonstrate this by plotting the difference in the cumulative reward obtained by DAS vs. one-step under the drug discovery $C = 10$ setting in Fig. 4. We see DAS collects fewer rewards at the beginning of the search as it spends its queries exploring the search space. As the search progresses, the policy transitions into a more exploitative behavior and ultimately ends up outperforming the myopic one-step policy. This trend is consistent with what has been observed from ENS-style policies in previous work (Jiang et al., 2017; 2018; Nguyen et al., 2021).

We use a logarithmic function to quantify the utility of discoveries from each target class, which balances recovery and diversity. However, one may reasonably look for other functions that better capture one’s preference (e.g., to encourage for either more recovery or more diversity, or to express different preferences across classes). We provide additional experimental results to further this discussion in Appx. C, and note that our approach can be easily extended to any positive and concave utility functions.

6. Conclusion

We have proposed a novel active search framework that rewards diverse discoveries and studied the problem from the Bayesian perspective. We first prove a hardness result analogous to one in the classical setting, showing the optimal policy cannot be approximated by a constant in polynomial time. We then propose a policy that simulates approximate optimal future queries in an efficient manner. This nonmyopic lookahead allows our algorithm to be aware of its remaining budget at any point during a search and thus trade off exploitation and exploration dynamically. Our experiments demonstrate the empirical success of our proposed policy with real-world datasets, and show that the policy is effective at building diverse datasets.

References

- Agarwal, S., Arora, H., Anand, S., and Arora, C. Contextual Diversity for Active Learning. In *European Conference on Computer Vision*, pp. 137–153. Springer, 2020.
- Auer, P. Using Confidence Bounds for Exploitation-Exploration Trade-offs. *Journal of Machine Learning Research*, 3:397–422, 2002.
- Bellman, R. *Dynamic Programming*. Princeton University Press, 1957.
- Benhenda, M. ChemGAN challenge for drug discovery: can AI reproduce natural chemical diversity? 2017. arXiv preprint arXiv:1708.08227 [stat.ML].
- Brinker, K. Incorporating Diversity in Active Learning with Support Vector Machines. In *Proceedings of the 20th International Conference on Machine Learning*, pp. 59–66, 2003.
- Citovsky, G., DeSalvo, G., Gentile, C., Karydas, L., Rajagopalan, A., Rostamizadeh, A., and Kumar, S. Batch Active Learning at Scale. *Advances in Neural Information Processing Systems 34*, 2021.
- Fouss, F., Pirotte, A., Renders, J.-M., and Saerens, M. Random-Walk Computation of Similarities between Nodes of a Graph with Application to Collaborative Recommendation. *IEEE Transactions on Knowledge and Data Engineering*, 19:355–369, 2007.
- Galloway, W. R., Isidro-Llobet, A., and Spring, D. R. Diversity-oriented synthesis as a tool for the discovery of novel biologically active small molecules. *Nature communications*, 1(1):1–13, 2010.
- Garnett, R. *Bayesian Optimization*. Cambridge University Press, 2022.
- Garnett, R., Krishnamurthy, Y., Xiong, X., Schneider, J., and Mann, R. Bayesian Optimal Active Search and Surveying. In *Proceedings of the 29th International Conference on Machine Learning*, 2012.
- Golovin, D. and Krause, A. Adaptive Submodularity: Theory and Applications in Active Learning and Stochastic Optimization. *Journal of Artificial Intelligence Research*, 42:427–486, 2011.
- Gu, Y., Jin, Z., and Chiu, S. C. Active learning combining uncertainty and diversity for multi-class image classification. *IET Computer Vision*, 9(3):400–407, 2015.
- Gupta, S., Shilton, A., Rana, S., and Venkatesh, S. Exploiting Strategy-Space Diversity for Batch Bayesian Optimization. In *Proceedings of the 21st International Conference on Artificial Intelligence and Statistics*, pp. 538–547, 2018.
- He, J. and Carbonell, J. Nearest-Neighbor-Based Active Learning for Rare Category Detection. In *Advances in Neural Information Processing Systems 20*, pp. 633–640, 2007.
- Jiang, S., Malkomes, G., Converse, G., Shofner, A., Moseley, B., and Garnett, R. Efficient Nonmyopic Active Search. In *Proceedings of the 34th International Conference on Machine Learning*, pp. 1714–1723, 2017.
- Jiang, S., Malkomes, G., Abbott, M., Moseley, B., and Garnett, R. Efficient nonmyopic batch active search. In *Advances in Neural Information Processing Systems 31*, pp. 1099–1109, 2018.
- Jiang, S., Garnett, R., and Moseley, B. Cost effective active search. In *Advances in Neural Information Processing Systems 32*, pp. 4880–4889, 2019.
- Krause, A. and Guestrin, C. Near-optimal Observation Selection using Submodular Functions. In *Proceedings of the 21st AAAI Conference on Artificial Intelligence*, pp. 1650–1654, 2007.
- Kulesza, A. and Taskar, B. Determinantal Point Processes for Machine Learning. *Foundations and Trends® in Machine Learning*, 5(2–3):123–286, 2012.
- Lin, C. H., Mausam, and Weld, D. S. Active Learning with Unbalanced Classes & Example-Generated Queries. In *Proceedings of the 6th AAAI Conference on Human Computation*, 2018.
- Liu, T., Lin, Y., Wen, X., Jorissen, R. N., and Gilson, M. K. BindingDB: A web-accessible database of experimentally determined protein–ligand binding affinities. *Nucleic acids research*, 35(suppl_1):D198–D201, 2007.
- Lukovic, M. K., Tian, Y., and Matusik, W. Diversity-Guided Multi-Objective Bayesian Optimization With Batch Evaluations. *Advances in Neural Information Processing Systems 33*, 33, 2020.
- Ma, L., Ding, B., Das, S., and Swaminathan, A. Active Learning for ML Enhanced Database Systems. In *Proceedings of the 2020 ACM SIGMOD International Conference on Management of Data*, pp. 175–191, 2020.
- Madani, O., Lizotte, D. J., and Greiner, R. Active Model Selection. In *Proceedings of the 20th Conference on Uncertainty in Artificial Intelligence*, pp. 357–365, 2004.
- Malkomes, G., Cheng, B., Lee, E. H., and Mccourt, M. Beyond the Pareto Efficient Frontier: Constraint Active Search for Multiobjective Experimental Design. In *Proceedings of the 38th International Conference on Machine Learning*, pp. 7423–7434, 2021.

- Mukadam, F., Nguyen, Q., Adrion, D. M., Appleby, G., Chen, R., Dang, H., Chang, R., Garnett, R., and Lopez, S. A. Efficient Discovery of Visible Light-Activated Azoarene Photoswitches with Long Half-Lives Using Active Search. *Journal of Chemical Information and Modeling*, 61(11):5524–5534, 2021.
- Nava, E., Mutn̄, M., and Krause, A. Diversified Sampling for Batched Bayesian Optimization with Determinantal Point Processes. 2021. arXiv preprint arXiv:2110.11665 [cs.LG].
- Nemhauser, G. L., Wolsey, L. A., and Fisher, M. L. An Analysis of Approximations for Maximizing Submodular Set Functions—I. *Mathematical Programming*, 14(1): 265–294, 1978.
- Nguyen, Q., Modiri, A., and Garnett, R. Nonmyopic Multifidelity Active Search. In *Proceedings of the 38th International Conference on Machine Learning*, pp. 8109–8118, 2021.
- Pereira, T., Abbasi, M., Ribeiro, B., and Arrais, J. P. Diversity oriented Deep Reinforcement Learning for targeted molecule generation. *Journal of Cheminformatics*, 13(1): 1–17, 2021.
- Rogers, D. and Hahn, M. Extended-Connectivity Fingerprints. *Journal of Chemical Information and Modeling*, 50(5):742–754, 2010.
- Sener, O. and Savarese, S. Active Learning for Convolutional Neural Networks: A Core-Set Approach. In *Proceedings of the 6th International Conference on Learning Representations*, 2018.
- Settles, B. Active Learning Literature Survey. Technical report, University of Wisconsin-Madison Department of Computer Sciences, 2009.
- Shu, L., Jiang, P., Shao, X., and Wang, Y. A New Multi-Objective Bayesian Optimization Formulation With the Acquisition Function for Convergence and Diversity. *Journal of Mechanical Design*, 142(9):091703, 2020.
- Sterling, T. and Irwin, J. J. Zinc 15–Ligand Discovery for Everyone. *Journal of Chemical Information and Modeling*, 55(11):2324–2337, 2015.
- Wang, Z., Garrett, C. R., Kaelbling, L. P., and Lozano-Pérez, T. Active model learning and diverse action sampling for task and motion planning. In *IEEE/RSJ International Conference on Intelligent Robots and Systems*, pp. 4107–4114, 2018.
- Warmuth, M. K., Rätsch, G., Mathieson, M., Liao, J., and Lemmen, C. Active Learning in the Drug Discovery Process. In *Advances in Neural Information Processing Systems 15*, pp. 1449–1456, 2002.
- Warmuth, M. K., Liao, J., Rätsch, G., Mathieson, M., Putta, S., and Lemmen, C. Active Learning with Support Vector Machines in the Drug Discovery Process. *Journal of Chemical Information and Computer Sciences*, 43(2): 667–673, 2003.
- Yang, Y., Ma, Z., Nie, F., Chang, X., and Hauptmann, A. G. Multi-Class Active Learning by Uncertainty Sampling with Diversity Maximization. *International Journal of Computer Vision*, 113(2):113–127, 2015.
- Zhdanov, F. Diverse mini-batch Active Learning. 2019. arXiv preprint arXiv:1901.05954 [cs.LG].

A. Hardness of Approximation

We present the proof of [Theorem 2.1](#). This is done by constructing a class of AS problems similar to those described in [Jiang et al. \(2017\)](#) but with different parameterizations. We sketch out the main arguments here, and refer to the supplementary materials of [Jiang et al. \(2017\)](#) for a complete description. Consider an AS problem whose setup is summarized in [Fig. 5](#) and described below. The problem has $n = 16^m$ points, where m is a free parameter, and the search budget is $T = 2^{m+1}$. Each of the n points is classified into two groups: “clumps” and “isolated points.”

The former consists of 4^m clumps, each of size T , and is visualized in [Fig. 5\(b\)](#). All points within the same clump share the same label, and exactly one clump contains positives. In each instance of the problem class being described, this positive clump is chosen uniformly at random among the 4^m clumps. As such, the prior marginal positive probability of any of these points is $p_{\text{clump}} = 4^{-m}$.

As for the isolated points, their labels are independent from one another. The marginal probability of an isolated is set to be $p_{\text{isolated}} = 1 - 0.5^{\frac{2m}{2m^2}}$. These isolated points are further separated into two categories:

- A secret set S of size $T/2 = 2^m$, visualized in [Fig. 5\(a\)](#), which encodes the location of the positive clump. The set S is first partitioned into $2m$ subsets S_1, S_2, \dots, S_{2m} , each of size $2^m/2m$. Each subset S_i encodes one virtual bit b_i of information about the location of S , and is further split into m groups of $2^m/2m^2$ points, with each group encoding a virtual bit b_{ij} by a logical OR. The aforementioned virtual bit b_i , on the other hand, is obtained via a logical XOR: $b_i = b_{i1} \oplus b_{i2} \oplus \dots \oplus b_{im}$.
- The remaining points, denoted as \mathcal{R} and visualized in [Fig. 5\(c\)](#), are completely independent from each other and any other points. We have $|\mathcal{R}| = 16^m - 2(8^m) - 2^m$.

We first make the same two observations as in [Jiang et al. \(2017\)](#).

Observation A.1. *At least m points from S_i need to be observed in order to infer one bit b_i of information about the location of the positive clump.*

Each b_{ij} has the same marginal probability of being 1:

$$\Pr(b_{ij} = 1) = 1 - \Pr(b_{ij} = 0) = 1 - (1 - p_{\text{isolated}})^{\frac{2^m}{2m^2}} = 0.5.$$

We also have $\Pr(b_i = 1) = 0.5$, as the positive clump is chosen uniformly at random. It is necessary to observe all virtual bits b_{ij} from the same group S_i to infer the bit b_i , since observing a fraction of the inputs of a XOR operator does not change the marginal belief about the output b_i . So, observing $(m - 1)$ or fewer points conveys no information about the positive clump.

Observation A.2. *Observing any number of clump points does not change the marginal probability of any point in the secret set S .*

The knowledge of b_i does not change the marginal probability of any b_{ij} . This is to say no point in S will have a different probability after observing b_i . This means observing points outside of S does not help distinguish S from the remaining isolated points in \mathcal{R} .

With this setup, we now compare the performance of the optimal policy and the expected performance of a given polynomial-time policy. To this end, we first consider the optimal policy with unlimited compute. Before querying any point, the policy computes the marginal probability of an arbitrary fixed clump point, conditioning on observing every possible subset of the isolated points of size m and fantasized positive labels. This set of $O(n^m)$ inference calls will reveal the location of the secret set S , as only points in S will update the probabilities of the fixed clump point.

Now the policy spends the first half of its budget querying S , the labels of which identify the positive clump. The policy now spends the second half of the budget collecting these positive points. The resulting reward, denoted as OPT, is lower-bounded in the worst-case scenario where S does not contain any positive point:

$$\text{OPT} \geq \log\left(1 + \frac{B}{2}\right) = \log(1 + 2^m).$$

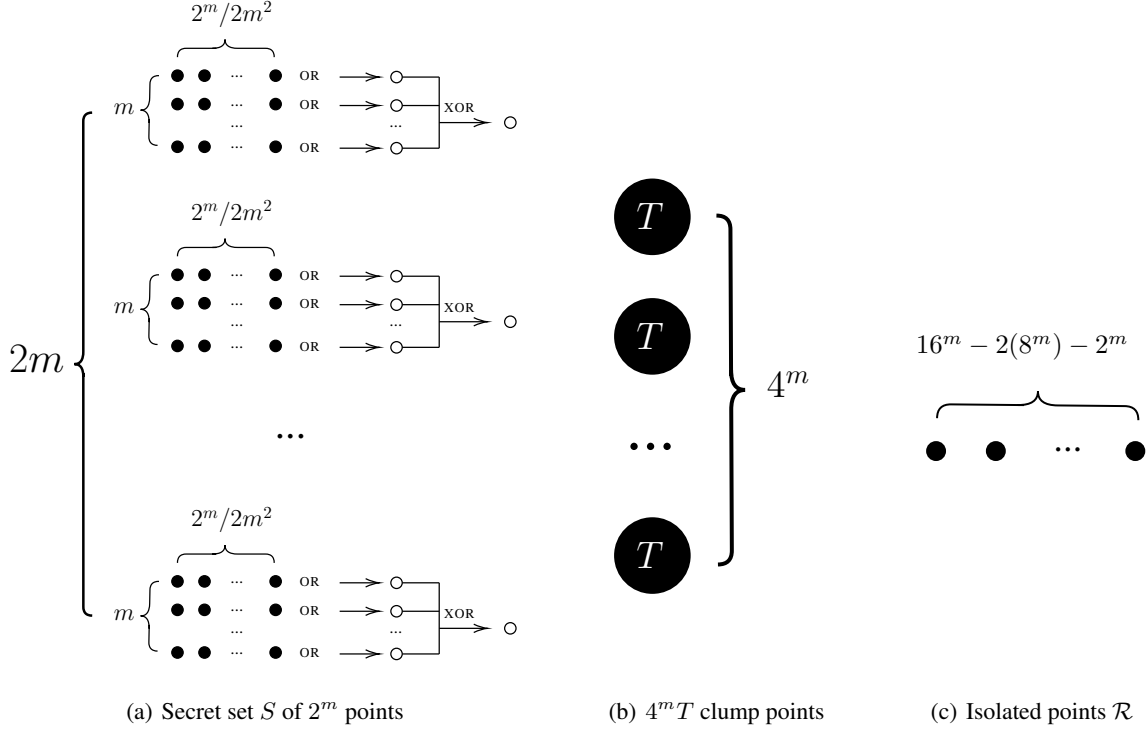


Figure 5. An instance of AS where any efficient algorithm can be arbitrarily worse than the optimal policy.

We now consider a policy \mathcal{A} . Let α denote the total number of inference calls performed by \mathcal{A} throughout its run. At the i^{th} inference call, \mathcal{A} uses a training set \mathcal{D}_i of size at most $B = 2^{m+1}$. We will show that \mathcal{A} has a very small chance of collecting a large reward by considering several cases.

We first examine the probability that \mathcal{A} finds the secret set S . By **Obs. A.1** and **A.2**, \mathcal{A} cannot differentiate between the points in S and those in \mathcal{R} unless $|\mathcal{D}_i \cap S| \geq m$. Suppose that before this inference call, the algorithm has no information about S (which is always true when $i = 1$). The chances of \mathcal{A} choosing \mathcal{D}_i such that $|\mathcal{D}_i \cap S| \geq m$ are no better than a random selection from $n - 2(8^m)$ isolated points. We can upper-bound the probability of this event by counting how many subsets of size 2^{m+1} would contain at least m points from S among all subsets of the $n - 2(8^m)$ isolated points:

$$\Pr(|\mathcal{D}_i \cap S| \geq m) \leq \frac{\binom{2^m}{m} \binom{n-2(8^m)-m}{2^{m+1}-m}}{\binom{n-2(8^m)}{2^{m+1}}}.$$

The RHS may further be upper-bounded by considering

$$\frac{\binom{2^m}{m} \binom{n-2(8^m)-m}{2^{m+1}-m}}{\binom{n-2(8^m)}{2^{m+1}}} = \frac{(2^m)! (n - 2(8^m) - m)! (2^{m+1})!}{m! (2^m - m)! (2^{m+1} - m)! (n - 2(8^m))!},$$

where

$$\frac{(2^m)!}{(2^m - m)!} < (2^m)^m; \quad \frac{(2^{m+1})!}{(2^{m+1} - m)!} < (2^{m+1})^m; \quad \frac{(n - 2(8^m) - m)!}{m! (n - 2(8^m))!} < \frac{1}{(n - 2(8^m))^m}.$$

The last inequality is due to

$$\frac{(n - 2(8^m))^m}{m!} < \frac{(n - 2(8^m))!}{(n - 2(8^m) - m)!},$$

which is true by observing that for each of the m factors on each side,

$$\frac{n - 2(8^m)}{i} < n - 2(8^m) - i + 1, \forall i = 1, \dots, m.$$

Overall, we upper-bound the probability that \mathcal{A} hits m points in S with

$$\Pr(|\mathcal{D}_i \cap S| \geq m) < \left(\frac{2^m 2^{m+1}}{n - 2(8^m)} \right)^m,$$

and union-bound the probability of \mathcal{A} “hitting” the secret set after α inferences, denoted as p_{hit} , with

$$p_{\text{hit}} < \frac{\alpha}{\left(\frac{n - 2(8^m)}{2^m 2^{m+1}} \right)^m}.$$

Here, $n - 2(8^m) = 16^m - 2(8^m) = \Theta(16^m)$, so

$$p_{\text{hit}} < \frac{\alpha}{\Theta\left(\left(\frac{16^m}{2(4^m)}\right)^m\right)} = \frac{\alpha}{\Theta(4^{m^2})}.$$

Hence, for any $\alpha = O(n^c) = O(16^{cm}) = O(4^{2cm})$, where c is a constant,

$$p_{\text{hit}} < O\left(\frac{4^{2cm}}{4^{m^2}}\right) = O(4^{-m^2}) = O(4^{-\log^2 n}).$$

In other words, the probability that \mathcal{A} does find the secret set S decreases as a function of n . Conditioned on this event, we upper-bound its performance with $\log(1 + 2^{m+1})$, assuming that every query is a hit.

On the other hand, if \mathcal{A} never finds S , we further consider the following subcases: if the algorithm queries an isolated point, no marginal probability is changed; if a clump point is queried, only the marginal probabilities of the points in the same clump are updated. The expected performance in these two cases can be upper-bounded by pretending that the algorithm had a budget of size $2T = 2^{m+2}$, half of which is spent on querying isolated points and half on clump points.

The expected utility after T queries on isolated points is $\mathbb{E}[\log(1 + X)]$, where $X = \sum_{i=1}^T X_i$ and $\Pr(X_i = 1) = p_{\text{isolated}}$. We further upper-bound this expectation using Jensen’s inequality:

$$\mathbb{E}[\log(1 + X)] < \log(\mathbb{E}[1 + X]) = \log(1 + T p_{\text{isolated}}) = \log\left(1 + 2^{m+1}(1 - 2^{-\frac{2^m}{2^{m^2}}})\right).$$

The expected utility after T queries on clump points is

$$\begin{aligned} \frac{\log(1 + T)}{4^m} + \left(1 - \frac{1}{4^m}\right) \left(\frac{\log T}{4^m - 1} + \left(1 - \frac{1}{4^m - 1}\right)(\dots)\right) &= \frac{\sum_{i=1}^T \log(1 + i)}{4^m} \\ &< \frac{T \log(1 + T)}{4^m} \\ &= \frac{\log(1 + 2^{m+1})}{2^{m-1}}. \end{aligned}$$

Combining the two subcases, we have the expected utility in the case where \mathcal{A} never hits S upper-bounded by

$$\log\left(1 + 2^{m+1}(1 - 2^{-\frac{2^m}{2^{m^2}}})\right) + \frac{\log(1 + 2^{m+1})}{2^{m-1}}.$$

With that, the overall expected utility of \mathcal{A} , denoted by $E_{\mathcal{A}}$ is upper-bounded by

$$E_{\mathcal{A}} < \log(1 + 2^{m+1}) p_{\text{hit}} + \log\left(1 + 2^{m+1}(1 - 2^{-\frac{2^m}{2^{m^2}}})\right) + \frac{\log(1 + 2^{m+1})}{2^{m-1}}.$$

We then consider the upper bound of the approximation ratio

$$\frac{E_{\mathcal{A}}}{\text{OPT}} < \frac{\log(1 + 2^{m+1})}{\log(1 + 2^m)} p_{\text{hit}} + \frac{\log\left(1 + 2^{m+1}\left(1 - 2^{-\frac{2^m}{2m^2}}\right)\right)}{\log(1 + 2^m)} + \frac{\log(1 + 2^{m+1})}{2^{m-1} \log(1 + 2^m)}.$$

The first and third terms are arbitrarily small with increasing m . As for the second term, L'Hôpital's rule shows that $1 - 2^{-\frac{2^m}{2m^2}} = \Theta\left(\frac{2m^2}{2^m}\right)$, so this term scales like $\Theta\left(\frac{\log(1+4m^2)}{\log(1+2^m)}\right)$, which is also arbitrarily small with increasing m . Thus, algorithm \mathcal{A} cannot approximate the optimal policy by a constant factor.

B. Batch Utility Approximation Quality

We run simulations to compare the performance of the Jensen's upper bound \bar{u} against Monte Carlo (MC) sampling. Using the CiteSeer^x dataset described in Sect. 5.1, we first construct \mathcal{D} by randomly selecting 50 points for each class ($|\mathcal{D}| = 50C$), and compute the posterior probabilities p_c with a k -NN to simulate a typical AS iteration. A random target batch X of size b is then chosen, and the considered approximation methods are applied on this batch. This entire procedure is repeated 10 times for each setting of (C, b) , and the average root mean squared error (RMSE) and time taken for each method to return are reported in Tabs. 2 and 3. (MC(s) denotes MC sampling using s samples.) Note that in settings with large C or b , exact computation of Eq. (4) is intractable, in which case MC (2^{15}) is used as the ground truth. Overall, our Jensen's approximation offers a good tradeoff between accuracy and speed.

C. Experiments on the Tradeoff Between Coverage and Recovery

A statistic that may be of interest in our multiclass AS problem is the *coverage* measure, defined to be the number of unique target classes discovered. If this measure is the search objective, the corresponding utility function assigns the first discovery in each class a reward of 1 and no reward for further discoveries of already-observed classes. At the other end of the spectrum is the diversity-blind objective in previous AS work (Garnett et al., 2012; Jiang et al., 2017), which only rewards recovery, i.e., the total number of discoveries. Our utility function balances between these two goals, giving positive but decreasing rewards. We only report the average of this utility in Sect. 5 but additionally find that DAS gives the highest coverage values under those experiments as well.

To offer further insight into the balance between coverage and recovery, we consider another AS problem introduced by Mukadam et al. (2021). The task is to search for molecular photoswitches with two specific desirable properties: high light absorbance and long half-lives. The collected dataset contains 2049 molecules, 733 of which are found to be targets according to the criteria defined in the study. Further, the authors partition the points into 29 groups by their respective substructures, thus defining a multiclass AS problem with $C = 30$ (a negative class and 29 positive classes). The number of targets in a class ranges from 0 to 121. We run our policies for $T = 100$, each for 20 repeats with random initial datasets, and report the average results in Tab. 4. We observe that this time, DAS gives the highest average utility but not the largest coverage. However, it balances between recovery and coverage and achieves reasonable scores for both.

Our logarithmic utility function might not capture one's true preference in some cases, and one may reasonably look for better-suited utility functions. In fact, any positive, concave function can be used to quantify the utility of discoveries from an individual target class. Then, one can flexibly control for how quickly rewards for additional discoveries decrease, which may even be dependent on the class. With that said, our analysis and decision-theoretic methods can be easily extended to this class of functions. The only requirements are positivity and concavity, both of which are natural properties of a search utility function.

Table 2. Quality and time of our approximation method against MC sampling, averaged across 10 random repeats of CiteSeer^x $C = 5$ experiments. Under each setting, the approximation with the lowest error (with respect to the chosen ground truth) is highlighted **bold**, and so is the fastest method.

Ground truth	RMSE					Time in seconds				
	Exact		MC(2^{15})			Exact		MC(2^{15})		
	b	3	10	30	100	300	3	10	30	100
Exact	-	-	NA	NA	NA	0.0031	53.7149	NA	NA	NA
MC(2^5)	0.0021	0.0027	0.0060	0.0090	0.0167	0.0026	0.0015	0.0021	0.0056	0.0195
MC(2^{10})	0.0004	0.0008	0.0014	0.0021	0.0025	0.0190	0.0304	0.0576	0.1574	0.4581
MC(2^{15})	0.0001	0.0001	-	-	-	0.4908	0.7933	1.7341	4.7440	14.4539
Ours	0.0001	0.0003	0.0010	0.0028	0.0059	0.0001	0.0003	0.0003	0.0003	0.0004

Table 3. Quality and time of our approximation method against MC sampling, averaged across 10 random repeats of CiteSeer^x $C = 10$ experiments. Under each setting, the approximation with the lowest error (with respect to the chosen ground truth) is highlighted **bold**, and so is the fastest method.

Ground truth	RMSE					Time in seconds				
	Exact		MC(2^{15})			Exact		MC(2^{15})		
	b	3	10	30	100	300	3	10	30	100
Exact	-	NA	NA	NA	NA	0.0056	NA	NA	NA	NA
MC(2^5)	0.0023	0.0056	0.0091	0.0141	0.0275	0.0008	0.0016	0.0022	0.0060	0.0178
MC(2^{10})	0.0005	0.0013	0.0010	0.0031	0.0032	0.0167	0.0281	0.0536	0.1522	0.4390
MC(2^{15})	0.0001	-	-	-	-	0.5122	0.8178	1.6678	4.7923	13.9236
Ours	0.0002	0.0007	0.0017	0.0055	0.0120	0.0003	0.0005	0.0004	0.0005	0.0007

Table 4. Average results across 20 experiments under the photoswitch dataset. The best performing policy under a given metric is highlighted **bold**.

	# hits	# unique classes	utility
ENS	94	2	5.04
RR-greedy	26	10	11.70
RR-UCB ($\beta^* = 3$)	26	10	11.70
RR-ENS	27	11	12.54
One-step	21	7	8.67
DAS (ours)	47	8	13.85